Proceedings of the ASME 2018 International Mechanical Engineering Congress & Exposition
IMECE 2018
November 9-15, 2018, Pittsburgh, PA, USA

IMECE2018-88249

MESOSCALE MATERIAL STRENGTH CHARACTERIZATION FOR USE IN FRACTURE MODELING

Katherine Acton*
Mechanical Engineering
University of St. Thomas
St. Paul, Minnesota 55105
Email: kacton@stthomas.edu

Bahador Bahmani
Reza Abedi
Mechanical, Aerospace & Biomedical Engineering
University of Tennessee Knoxville (UTK) /
Space Institute (UTSI)
Tullahoma, Tennessee, 37388
Email: bbahmani@vols.utk.edu
rabedi@utk.edu

ABSTRACT

To accurately simulate fracture, it is necessary to account for small-scale randomness in the properties of a material. Apparent properties of Statistical Volume Elements (SVE), can be characterized below the scale of a Representative Volume Element (RVE). Apparent properties cannot be defined uniquely for an SVE, in the manner that unique effective properties can be defined for an RVE. Both constitutive behavior and material strength properties in SVE must be statistically characterized. The geometrical partitioning method can be critically important in affecting the probability distributions of mesoscale material property parameters. Here, a Voronoi tessellation based partitioning scheme is applied to generate SVE. Resulting material property distributions are compared with those from SVE generated by square partitioning. The proportional limit stress of the SVE is used to approximate SVE strength. Superposition of elastic results is used to obtain failure strength distributions from boundary conditions at variable angles of loading.

INTRODUCTION

When a material is modeled as homogeneous in a fracture simulation, the simulation will not accurately capture the small scale randomness inherent in crack propagation due to microstructural heterogeneity. However, direct simulation of material flaws, defects, pores or inclusions may be infeasible due to computational expense, and/or material characterization may not be available in sufficient detail. Therefore, probabilistic continuum models are needed that accurately characterize both material properties and variability in material properties at a relatively small scale. Traditional Representative Volume Element (RVE) approaches in modeling heterogeneous material provide a continuum approximation, but obscure local material variability. Statistical Volume Element (SVE) approaches provide a continuum approximation of material properties at a mesoscale. Where d is the length scale of a typical microstructural feature (e.g. inclusion radius), and L is the macroscopic scale of the structure, the size of the SVE and RVE (l_{SVE} and l_{RVE} respectively) are ordered as follows:

$$d < l_{SVE} < l_{RVE} \ll L \quad (1)$$

A principle challenge with SVE approaches is the non-uniqueness of material properties obtained at a scale below the scale of an RVE. Extensive literature is devoted to the dependency of SVE apparent properties on the boundary conditions used to obtain the stress strain relationship [1–6]. SVE can be used to generate statistical characterizations of random fields of material properties, which can be performed for use in stochastic

*Address all correspondence to this author.

simulation [7–10]. Often, analysis of the accuracy of SVE material properties is considered as a function of SVE size. Increasing the size of an SVE increases the accuracy of elastic results. However, whether a phenomenological model such as Weibull model [?] is used [?, ?], or strength is directly characterized by SVEs [?, ?] the material inhomogeneity is lost at larger representation/averaging sizes. Moreover, strength properties tend to decrease as the size of an SVE increases, a phenomenon known as the *size effect*. To limit the size effect and maintain fracture strength inhomogeneities—which are particularly important for fragmentation studies [?, ?]—unlike elastic results, it is thus preferred to limit the use of large scale SVE (and RVE) for strength predictions.

SVE partition shape influences the determination of individual SVE properties, as well as statistics drawn from a population of SVE that partition an RVE. Partitioning a microstructure with inclusions into collections of Voronoi cells has been shown to provide an advantage over square partitioning [11, 12]. Using Voronoi cell partitioning, inclusions do not intersect partition boundaries, avoiding the introduction of spurious stress concentrations. Based on this observation, previous work has focused on comparison of elastic material property statistics obtained by square and Voronoi partitioning. The current work extends previous results to focus on comparison of material strength properties obtained by square and Voronoi partitioning. In particular, the dependence of material strength on the angular direction of loading is investigated. The angular dependence of strength is important to statistically characterize, as it affects directionality of crack propagation in a fracture analysis.

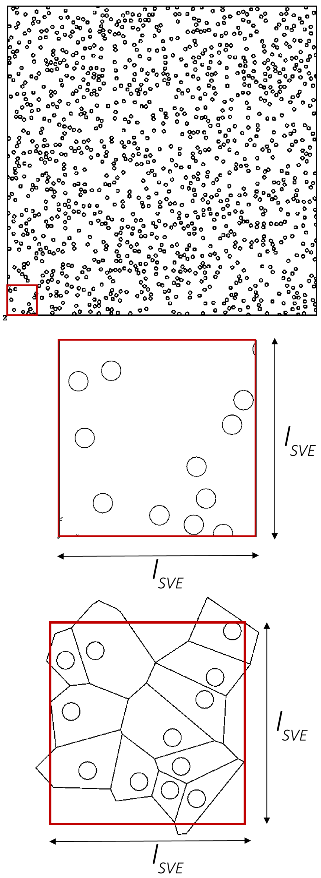

FIGURE 1. PARTITIONING OF RVE MICROSTRUCTURE (TOP) INTO SQUARE AND VORONOI SVE (MIDDLE AND BOTTOM FIGURES, RESPECTIVELY) EACH WITH SIDE LENGTH S.

SQUARE AND VORONOI PARTITIONING OF SVE

A typical square and Voronoi partitioning of an RVE is shown in Fig. 1. In this illustration, the side length s of the SVE is ten times the length of the inclusion diameter. In general, a nondimensional parameter δ is defined to characterize SVE size, given as:

$$\delta = l_{SVE}/d \tag{2}$$

with variables as defined in Eq. 1. In this work, the diameter of all inclusions is a unit value, and the side length of the square RVE is considered to be $l_{RVE} = 100d$. To create SVE, the RVE side length is partitioned by powers of two ($\frac{1}{4}, \frac{1}{8}, \frac{1}{16}, \frac{1}{32}$) to generate SVE with sizes $\delta = 25, 12.5, 6.25, 3.125$, respectively.

Square partitioning is a straightforward method that ensures each SVE will be of uniform area, although partition boundaries often intersect inclusions, as shown in the figure. Voronoi partitioning is based on an underlying square partition of the RVE. In a given square region, if the centroid of a Voronoi cell lies within this region, the cell is assigned to the corresponding SVE. This leads to SVE with areas that have relatively high variation at small SVE sizes, and relatively low variation at large SVE sizes. As shown in the figure, the Voronoi cell partitioning approach does not allow inclusions to intersect partition boundaries. For more details on the partitioning method used in this analysis, see [12, 13].

DETERMINATION OF SVE FAILURE STRENGTH

Material properties determined on an SVE are non-unique, and depend on applied boundary conditions. In this work, a set of mixed uniform boundary conditions is applied, with displacement conditions in plane in 2D elements under plane stress. Superposition is used to combine hydrostatic, pure and simple shear boundary conditions (denoted H, P, and S) such that these results can be used to span the space of applied strains. This process, and the method for determining failure strength as a function of load angle, are briefly summarized here, and explained in more detail in [13].

With a known uniform strain condition applied at the boundary of the SVE for each of the three principle loading directions, the average stress in the SVE is then calculated using FEA. Using the prescribed strain/average stress relationship for *H,P* and *S* strains, a stiffness matrix is calculated for each SVE.

The maximum stress at the matrix-inclusion boundary, in the direction normal to the inclusion, is also found for each SVE under *H,P* and *S* applied loading. Results are superposed to generate results for normal and shear load applied from angles of zero through 180 degrees. A threshold value σ^{TH} is set, such that when this value is exceeded at the matrix-inclusion interface, the material has reached an elastic limit signifying failure. Although this is not the ultimate fracture strength, for brittle and quasi-brittle materials, this threshold value is shown to be a close approximation for quasi-static [**?**] and low-rate dynamic loadings [**?**]. The same assumption is used in prior work for microcracked domains [?] and random composites [?, 13].

The point at which the maximum matrix-inclusion boundary stress reaches the threshold value is calculated for two specific cases at each load angle θ. First, as shown in Fig. 2, the average normal SVE stress is fixed to have a unit value, with zero average shear stress. In this case, the strength value $\tilde{s}_n$ is calculated, that can be multiplied by the maximum matrix inclusion interface stress to achieve the threshold value σ^{TH}. This value $\tilde{s}_n$ is considered the normal strength of the SVE. Similarly, enforcing an average shear stress with unit value and average normal stress equal to zero yields an approximation of $\tilde{s}_t$, the SVE shear strength.

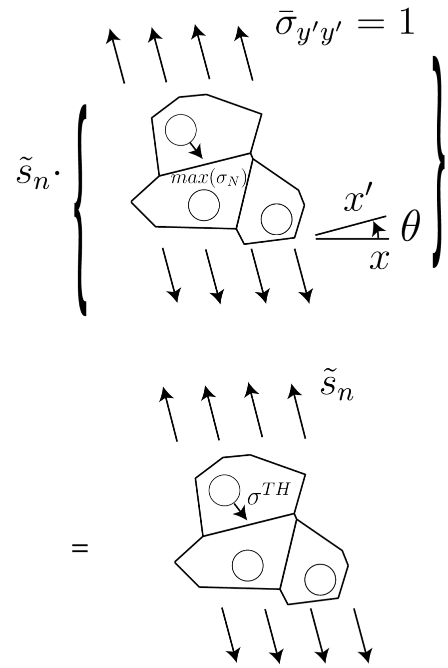

FIGURE 2. CALCULATION OF FAILURE STRENGTH $\tilde{s}_n$. FAILURE OCCURS WHEN THE MAXIMUM STRESS ON ANY INCLUSION BOUNDARY, IN THE DIRECTION NORMAL TO THE INCLUSION, REACHES A THRESHOLD VALUE σ^{TH} [13].

RESULTS

Results are presented showing convergence of material properties as a function of partition size for SVE generated using square and Voronoi partitioning. Results are also presented showing the dependence of strength properties on angle of loading for square and Voronoi SVE.

Convergence of Material Properties

Figures 3, 4 and 5 show the convergence of material bulk modulus κ, normal strength $\tilde{S}_n$ and shear strength $\tilde{S}_t$, respectively, as a function of SVE size for square partitioned SVE. Figures 6, 7 and 8 show the convergence of material bulk modulus, normal strength and shear strength, respectively, as a function of SVE size for Voronoi partitioned SVE. In each case, the mean material property is plotted within an envelope showing range of the minimum and maximum values recovered for SVE of a given size.

In all cases, convergence of mean, minimum and maximum values is observed with increasing window size. This is expected, as larger window sizes approach the size of an RVE. All results showing material strength (Figs. 4, 5, 7 and 8) show a trend of decreasing material strength with increasing SVE size. This is also expected, as larger SVEs have a higher likelihood of containing regions with large stress concentration, and therefore lower strength.

In all cases, convergence is improved by Voronoi partitioning. Small window sizes predict mean values closer to those predicted by large window sizes for the Voronoi partitioning method. The minimum and maximum material property values are closer, even at small window sizes, for SVEs partitioned using the Voronoi method.

Material Property Dependence on Angle of Loading

Results showing the dependence of SVE material properties on the angle of applied load are considered for square and Voronoi SVE of relatively large and small sizes ($\delta = 12.5$ and $\delta = 3.125$). In each case, either the normal strength ($\tilde{s}_n$) or the shear strength ($\tilde{s}_t$) is divided by the threshold value of stress (σ^{TH}). Note that $\tilde{S}_n$ shown in Fig. 4 and 7, is the mean value of the angle-dependent SVE fracture strength $\tilde{s}_n(\theta)$ over angle θ; that is $\tilde{S}_n = \text{mean}_{\theta\in[0,\ \pi]}\tilde{s}_n(\theta)$. Similarly, $\tilde{S}_t = \text{mean}_{\theta\in[0,\ \pi]}\tilde{s}_t(\theta)$. The threshold stress is defined above as the maximum stress the

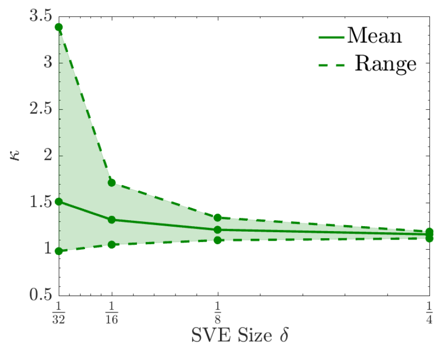

FIGURE 3. BULK MODULUS κ AS A FUNCTION OF SVE SIZE FOR SQUARE SVE.

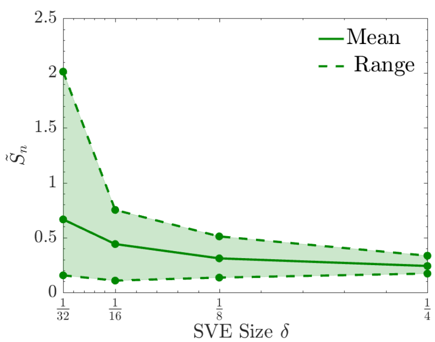

FIGURE 4. NORMAL STRENGTH $\tilde{S}_n$ AS A FUNCTION OF SVE SIZE FOR SQUARE SVE.

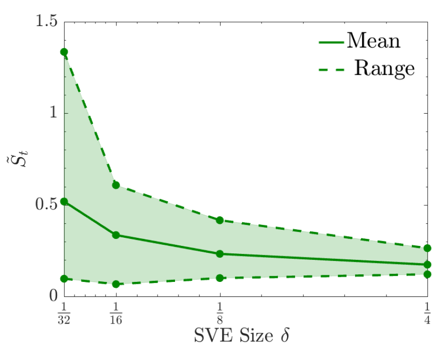

FIGURE 5. SHEAR STRENGTH $\tilde{S}_t$ AS A FUNCTION OF SVE SIZE FOR SQUARE SVE.

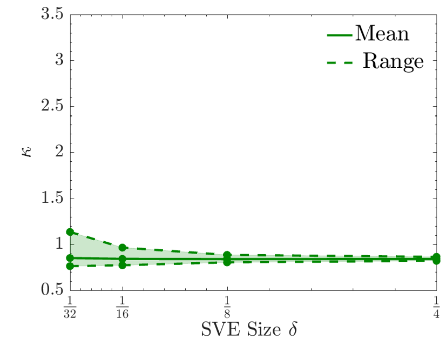

FIGURE 6. BULK MODULUS κ AS A FUNCTION OF SVE SIZE FOR VORONOI SVE.

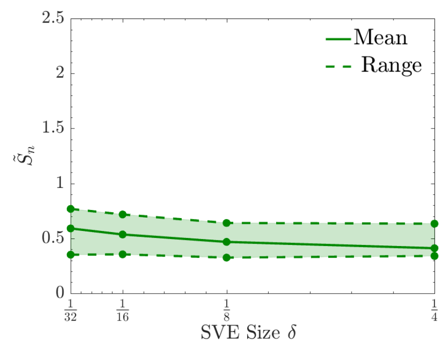

FIGURE 7. NORMAL STRENGTH $\tilde{S}_n$ AS A FUNCTION OF SVE SIZE FOR VORONOI SVE.

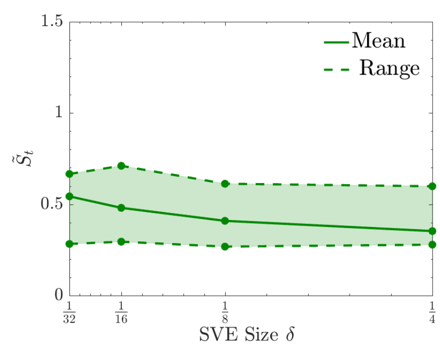

FIGURE 8. SHEAR STRENGTH $\tilde{S}_t$ AS A FUNCTION OF SVE SIZE FOR VORONOI SVE.

matrix may reach at the matrix/inclusion boundary, in the direction normal to the inclusion, before failure is assumed. These normalized values are plotted for small and large square SVE (Figs. 9 through 12), and small and large Voronoi SVE (Figs. 13 through 16).

Results show that material property anisotropy often corresponds to the angle of loading applied. Relative extrema tend to occur in both normal and shear strength in all square SVE, and the larger size Voronoi SVE, when $\theta = 0^\circ, 45^\circ, 90^\circ, 135^\circ$ and 180° (Figs. 9 through 14). Considering the applied loading (see

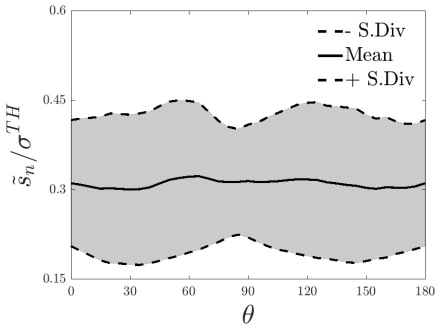

FIGURE 9. NORMALIZED NORMAL STRENGTH AS A FUNCTION OF LOADING ANGLE θ FOR SQUARE SVE SIZE $\delta = 12.5$

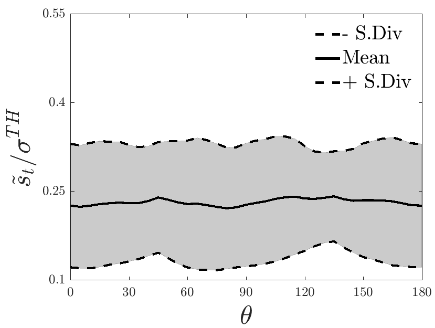

FIGURE 10. NORMALIZED SHEAR STRENGTH AS A FUNCTION OF LOADING ANGLE θ FOR SQUARE SVE SIZE $\delta = 12.5$

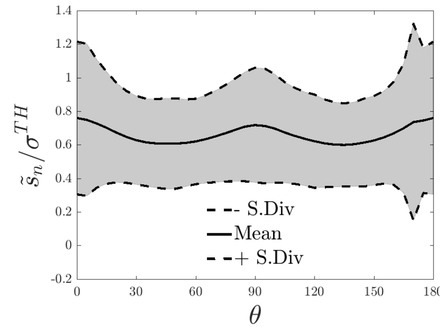

FIGURE 11. NORMALIZED NORMAL STRENGTH AS A FUNCTION OF LOADING ANGLE θ FOR SQUARE SVE SIZE $\delta = 3.125$

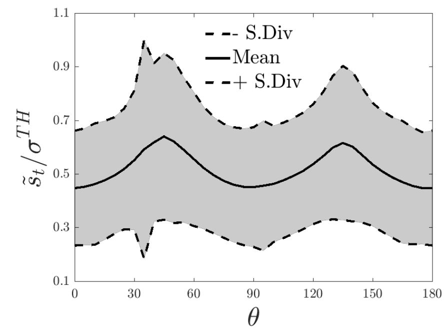

FIGURE 12. NORMALIZED SHEAR STRENGTH AS A FUNCTION OF LOADING ANGLE θ FOR SQUARE SVE SIZE $\delta = 3.125$

Fig. 2), where the SVE has square boundaries (or in the case of the large size Voronoi SVE, *relatively* square boundaries), these are angles where loading is aligned with SVE geometry. Only in the small size Voronoi SVE (Figs. 15 and 16) do the SVEs display isotropy, or independence between the material strength properties recovered, and the applied angle of loading. At a small length scale, the Voronoi SVE are not square, but rather polygonal configurations such as the one pictured in Fig. 2. In these SVE, the boundaries are nearly randomly aligned with respect to the angle of loading.

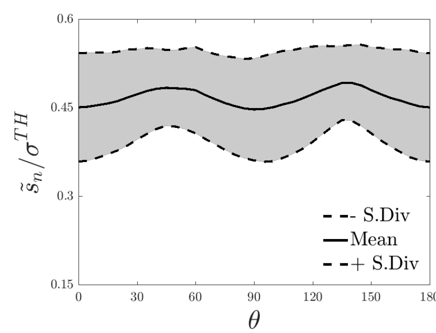

FIGURE 13. NORMALIZED NORMAL STRENGTH AS A FUNCTION OF LOADING ANGLE θ FOR VORONOI SVE SIZE $\delta = 12.5$

CONCLUSIONS

Results of this work highlight the utility of SVE homogenization methods based on Voronoi cell partitioning. Both elastic properties and strength properties are shown to converge more rapidly with increasing SVE size when Voronoi partitioning is used. This suggests that wide scatter in recovered material properties at small window sizes may often be due to stress concentrations on the boundaries of the SVE when inclusions intersect these partition boundaries. Eliminating this type of stress concentration gives a more accurate representation of the true variability of recovered properties due to geometric variation in material microstructure.

It is also shown that square SVE, or square-like SVE (such as large clusters of Voronoi cells chosen based on an underlying square boundary), predict greater material anisotropy. This

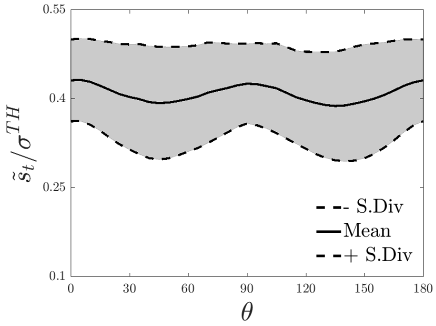

FIGURE 14. NORMALIZED SHEAR STRENGTH AS A FUNCTION OF LOADING ANGLE θ FOR VORONOI SVE SIZE $\delta = 12.5$

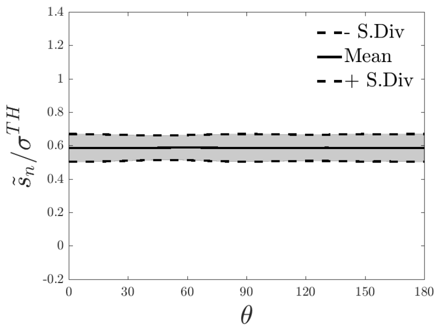

FIGURE 15. NORMALIZED NORMAL STRENGTH AS A FUNCTION OF LOADING ANGLE θ FOR VORONOI SVE SIZE $\delta = 3.125$

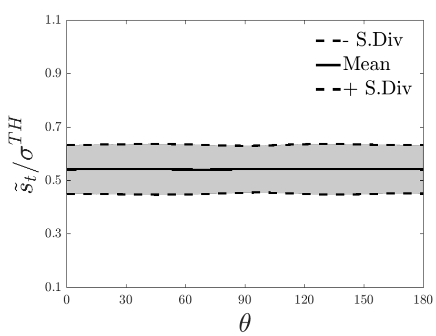

FIGURE 16. NORMALIZED SHEAR STRENGTH AS A FUNCTION OF LOADING ANGLE θ FOR VORONOI SVE SIZE $\delta = 3.125$

anisotropy is not due to actual material anisotropy, but rather to the alignment of SVE boundaries with the direction of applied loading on the SVE. This highlights the fact that SVE apparent properties are non-unique (unlike RVE effective properties), and depend on the choice of loading. SVE partitions based on collections of Voronoi cells can be used to reduce some of the variability in recovered properties due to spurious effects, such as the presence of stress concentrations on the SVE boundary, and the alignment of SVE geometry with direction of applied load. Statistics based on these SVEs are more accurate to be used as the basis to simulate brittle fracture.

ACKNOWLEDGMENT

The authors acknowledge support from the U.S. National Science Foundation (NSF), CMMI - Mechanics of Materials and Structures (MoMS) program, grant number 1538332. Supplemental funding from this award through a Research Opportunity Award (ROA) also supported research at the University of St Thomas.

REFERENCES

[1] Hazanov, S., and Huet, C., 1994. "Order relationships for boundary conditions effect in heterogeneous bodies smaller than the representative volume". *Journal of the Mechanics and Physics of Solids,* ***42***(12), pp. 1995–2011.

[2] Huet, C., 1990. "Application of variational concepts to size effects in elastic heterogeneous bodies". *Journal of the Mechanics and Physics of Solids,* ***38***(6), pp. 813–841.

[3] Ostoja-Starzewski, M., 2006. "Material spatial randomness: From statistical to representative volume element". *Probabilistic Engineering Mechanics,* ***21***(2), pp. 112–132.

[4] Ostoja-Starzewski, M., 1998. "Random field models of heterogeneous materials". *International Journal of Solids and Structures,* ***35***(19), pp. 2429–2455.

[5] Gitman, I. M., Askes, H., and Sluys, L. J., 2007. "Representative volume: Existence and size determination". *Engineering Fracture Mechanics,* ***74***(16), pp. 2518–2534.

[6] Kanit, T., Forest, S., Galliet, I., Mounoury, V., and Jeulin, D., 2003. "Determination of the size of the representative volume element for random composites: statistical and numerical approach". *International Journal of Solids and Structures,* ***40***(13), pp. 3647–3679.

[7] Baxter, S., and Graham, L., 2000. "Characterization of random composites using moving-window technique". *Journal of Engineering Mechanics,* ***126***(4), pp. 389–397.

[8] Graham, L., and Baxter, S., 2001. "Simulation of local material properties based on moving-window gmc". *Probabilistic Engineering Mechanics,* ***16***(4), pp. 295–305.

[9] Graham-Brady, L., Siragy, E., and Baxter, S., 2003. "Analysis of heterogeneous composites based on moving-window techniques". *Journal of engineering mechanics,* ***129***(9), pp. 1054–1064.

[10] Acton, K., and Graham-Brady, L., 2009. "Meso-scale modeling of plasticity in composites". *Computer Methods in Applied Mechanics and Engineering,* ***198***(9), pp. 920–932.

[11] Weibull, W., 1951. "A statistical distribution function of

wide applicability". *Journal of Applied Mechanics,* ***18***, pp. 293–297.

[12] Abedi, R., Omidi, O., and Clarke, P., 2016. "Numerical simulation of rock dynamic fracturing and failure including microscale material randomness". In Proceeding: 50th US Rock Mechanics/Geomechanics Symposium. ARMA 16-0531.

[13] Abedi, R., Haber, R. B., and Clarke, P. L., 2017. "Effect of random defects on dynamic fracture in quasi-brittle materials". *International Journal of Fracture,* ***208***(1-2), pp. 241–268.

[14] Koyama, T., and Jing, L., 2007. "Effects of model scale and particle size on micro-mechanical properties and failure processes of rocks—a particle mechanics approach". *Engineering Analysis with Boundary Elements,* ***31***(5), pp. 458–472.

[15] Acton, K., Baxter, S., Bahmani, B., Clarke, P., and Abedi, R., November 3-9, 2017. "Mesoscale models characterizing material property fields used as a basis for predicting fracture patterns in quasi-brittle materials". In Proceedings of ASME 2017 International Mechanical Engineering Congress & Exposition IMECE 2017, pp. V009T12A061, 5 pages. IMECE2017-71500.

[16] Clarke, P., Abedi, R., Bahmani, B., Acton, K., and Baxter, S., 2017. "Effect of the spatial inhomogeneity of fracture strength on fracture pattern for quasi-brittle materials". In Proceedings of ASME 2017 International Mechanical Engineering Congress & Exposition IMECE 2017, p. V009T12A045 (9 pages). IMECE2017-71515.

[17] Salmi, M., Auslender, F., Bornert, M., and Fogli, M., 2012. "Apparent and effective mechanical properties of linear matrix-inclusion random composites: Improved bounds for the effective behavior". *International Journal of Solids and Structures,* ***49***(10), pp. 1195–1211.

[18] Acton, K. A., and Baxter, S. C., 2017. "Characterization of random composite properties based on statistical volume element partitioning". *Journal of Engineering Mechanics,* ***144***(2), p. 04017168.

[19] Acton, K. A., Baxter, S. C., Bahmani, B., Clarke, P. L., and Abedi, R., 2018. "Voronoi tessellation based statistical volume element characterization for use in fracture modeling". *Computer Methods in Applied Mechanics and Engineering,* ***336***, pp. 135–155.

[20] Nguyen, V. P., Lloberas-Valls, O., Stroeven, M., and Sluys, L. J., 2011. "Homogenization-based multiscale crack modelling: From micro-diffusive damage to macro-cracks". *Computer Methods in Applied Mechanics and Engineering,* ***200***(9), pp. 1220–36.

[21] Daphalapurkar, N., Ramesh, K., Graham-Brady, L., and Molinari, J., 2011. "Predicting variability in the dynamic failure strength of brittle materials considering pre-existing flaws". *Journal of the Mechanics and Physics of Solids,* ***59***(2), pp. 297–319.